

20 **Abstract**

21 **Background** – Obesity is a serious risk factor for cardiovascular diseases. A high fat diet
22 results in cellular oxidative stress and endothelial dysfunction in resistance-sized arteries,
23 characterized by reduced nitric oxide (NO) and endothelium-dependent hyperpolarizing
24 (EDH) responses. Thioredoxin-1, a sulfo-oxidoreductase protein that cleaves disulfide
25 bridges between two adjacent cysteine residues in oxidized proteins, has been shown to
26 lower blood pressure and improve endothelium-dependent relaxing responses in aged
27 C57Bl6/J mice.

28 **Methods and Results** – Young (~ 3 month-old) male C57Bl6/J mice were fed a high fat
29 diet (42% kcal from fat; obese) or a normal chow (lean) for 3 months. Mice were
30 administered recombinant human thioredoxin-1 (rhTrx; 25 mg/kg) or saline (0.9% NaCl)
31 via tail vein injection at the start, after one month, and after two months. Body weight
32 (BW) was comparable between lean/rhTrx1 and lean/saline at the time of euthanasia (32
33 \pm 1 g versus 32 \pm 1 g). The high fat regimen resulted in a comparable BW between
34 obese/saline and obese/rhTrx mice (47 \pm 1 g versus 45 \pm 2 g, respectively). Small
35 (second-order branches) mesenteric arteries (MA2), coronary and femoral arteries were
36 isolated and mounted on the wire-myograph. MA2 and femoral arteries from obese/saline
37 had blunted acetylcholine (10^{-9} – 10^{-5} M)-mediated relaxations compared to lean/saline
38 mice, but not to the NO donor sodium nitroprusside. NO and EDH-mediated relaxing
39 responses were blunted in MA2 from obese/lean mice compared to the three other
40 groups.

41 **Conclusion** – Tail vein injections with rhTrx prevented endothelial dysfunction in obese
42 mice by improving NO and EDH relaxing responses in MA2.

43 In resistance-sized arteries ($< 250 \mu\text{m}$ in lumen diameter) relaxation is mediated via
44 endothelium-derived factors such as NO and prostacyclin (PGI_2), but also by a conductive
45 electro-coupled pathway, called endothelium-dependent hyperpolarization (EDH), that is
46 associated with a propagation of endothelial and smooth muscle cell hyperpolarization
47 [1]. Endothelial calcium-activated potassium channels (K_{Ca}) initiate and propagate this
48 EDH response [1]. In the endothelium of small mesenteric arteries, small-conductance
49 K_{Ca} (SK_{Ca}) and intermediate-conductance K_{Ca} (IK_{Ca}) are solely responsible for this EDH
50 [2]. In isometric wire-myography this EDH can be assessed in a contracted artery
51 segment followed by endothelial K_{Ca} opening under conditions where NO and PGI_2
52 release is inhibited. Under pathological conditions, including obesity, the contribution of
53 these endothelium-derived mediators is compromised (for a review see [3, 4]). An altered
54 cellular reduction-oxidation (redox) balance shifted towards a more oxidative state is
55 presumed to be the culprit of this endothelial dysfunction [5, 6]. Thiol/disulfide redox
56 changes of specific amino acids, most notably cysteine, modulate the activity of many
57 enzymes [7]. Thioredoxin-1 (Trx) is a 12-kDa cytosolic oxidoreductase capable of
58 reducing disulfide bridges between two adjacent cysteine residues, hereby keeping
59 cysteine groups in its active thiol (reduced) formation [8]. Overexpression of human Trx
60 in mice has been elegantly shown to reduce age-related hypertension [9], to increase
61 endothelium-dependent acetylcholine-mediated relaxations in the mesenteric vascular
62 bed [9, 10] and to preserve endothelial nitric oxide synthase (eNOS) activity via a
63 reductive deglutathionylation process [11]. In addition, the EDH response was enhanced
64 in small mesenteric arteries derived from these Trx transgenic mice compared to their
65 wild-type littermates [10]. These observations suggest that Trx maintains the activity of

66 eNOS and endothelial K_{Ca} channels. In this study it was hypothesized that tail vein
67 injections of recombinant human Trx (rhTrx) would protect against a high fat diet-induced
68 impairment in endothelium-dependent relaxation in resistance-sized arteries in C57Bl6/J
69 mice. In this study, attention was focused on the role of endothelium-derived NO and EDH
70 relaxing responses in mediating ACh- and NS309-induced relaxations in murine arteries
71 derived from lean and obese mice with or without intervention with rhTrx.

72 **Methods**

73 **Animals and tail vein injections**

74 Male C57Bl6/J mice (10 – 12 weeks) were placed on either a normal chow (lean group)
75 or a high fat diet (obese group). The high fat (42% kcal from fat) diet was purchased from
76 Harlan Laboratories (Teklad Custom Research Diet TD.88137). Mice were divided in four
77 groups: lean/saline, obese/saline, lean/rhTrx, and obese/rhTrx. In the saline groups, mice
78 were injected via the tail vein with saline (100 μ L of a 0.9% NaCl sterile solution), and for
79 the rhTrx group with recombinant human Thioredoxin-1 (R&D Systems; 2.5 mg/kg in 100
80 μ L solution in 0.9% NaCl solution). Mice were briefly placed in a holding chamber and
81 anesthetized with isoflurane (1.5% delivered in 100% O₂). The tail was heated with a light
82 source in order to dilate the tail vein. Tail vein injections were performed with insulin
83 syringes (Exel, 30G). After one and two months the tail vein injections were repeated.
84 After three months mice were euthanized. All procedures were approved by the IACUC
85 at Campbell University and were consistent with the *Guide for the Care and Use of*
86 *Laboratory Animals* published by the National Institute of Health. All animals were
87 maintained on a standard 12-h light/12-h dark cycle, in a temperature-controlled barrier
88 facility.

89 **Isolation of arteries and isometric wire-myography**

90 Mice were euthanized via CO₂ inhalation and the mesentery and heart were dissected.
91 From the left upper leg a 2 mm segment of the femoral artery was dissected. The
92 mesentery was placed in a Petri dish fill with black silicon and ice-cold Krebs Ringer Buffer
93 (KRB) with the following composition (in mM): 118.5 NaCl, 4.7 KCl, 2.5 CaCl₂, 1.2 MgSO₄,

94 1.2 KH₂PO₄, 25.0 NaHCO₃, and 5.5 D-glucose. Second-order branches of the superior
95 mesenteric artery (MA2) were dissected. From the heart a 1.5 – 2 mm-segment of the left
96 descending coronary artery was dissected. Segments were mounted on a wire-myograph
97 (Danish Myotechnology Inc, Model 620M, Aarhus, Denmark) and stretched to their
98 optimal internal circumference as described earlier [9]. Force (mN) generated by stretch
99 was corrected for vessel length to obtain tension values in mN/mm. Vessel length was
100 measured in the myograph chamber with the help of a scale bar in the ocular of the stereo
101 dissecting microscope. After an incubation period of 60 minutes, arteries were “woken
102 up” by replacing KRB with 60 mM KCl in KRB (replacing equimolar NaCl with KCl), thus
103 generating a stable tension after a few minutes. This tension level (minus the baseline
104 tension) was set as 100% contraction (as % of K₆₀). Cumulative concentration-response
105 curves (CRC) were performed with phenylephrine (PHE; 0.01 – 30 μM) for MA2, and
106 serotonin (5-HT; 0.001 – 3 μM) for coronary and femoral arteries. Cumulative CRC to
107 acetylcholine (ACh; 0.001 – 10 μM) were assessed in contracted artery segments in the
108 absence of any inhibitors. Endothelium-independent relaxations were assessed with CRC
109 to the NO donor sodium nitroprusside (0.1 nM – 10 μM) in the presence of the non-
110 selective NO synthase blocker N^o-nitro-L-arginine methyl ester (L-NAME; 100 μM) and
111 the non-selective cyclo-oxygenase inhibitor indomethacin (10 μM).

112 **Protocol to isolate the contribution of NO in PHE-induced contractions and ACh-**
113 **induced relaxing responses in MA2**

114 The contribution of NO in PHE-induced contractions and ACh-induced relaxations was
115 assessed by comparing the area between the curves (ABC) of the individual
116 concentration-response curves (CRCs) in the absence and presence of the L-NAME. To

117 rule out any contribution of vasoactive prostaglandins, all segments were treated with
118 indomethacin in the remainder of this study.

119 **Protocol to isolate the contribution of EDH in ACh- and NS309-induced relaxing**
120 **responses in MA2**

121 The EDH response was blocked with selective inhibitors of small-conductance and
122 intermediate-conductance calcium-activated potassium channels (SK_{Ca} and IK_{Ca},
123 respectively) by UCL-1684 (1 μM) and TRAM-34 (10 μM), respectively. Both inhibitors
124 were incubated for 30 minutes prior CRC to ACh. The EDH-mediated relaxing responses
125 were assessed by calculating ABC between the individual CRCs to ACh and the direct
126 endothelial K_{Ca} opener NS309 [12] in the absence and presence of TRAM-34 and UCL-
127 1684. Another protocol was designed to assess EDH responses in MA2 that were
128 incubated with L-NAME. The remaining relaxing responses to ACh and NS309 is an
129 indication for the contribution of the EDH response in the absence of NO and vasoactive
130 prostaglandins.

131 **Data and statistical analysis**

132 Data are shown as mean ± SEM. Concentration-response curves were analyzed with
133 two-way analysis of variance (ANOVA) followed by Bonferroni post-hoc test or Tukey's
134 test for multiple comparisons. Other values were analyzed by paired and unpaired
135 Student's *t* test. *P* < 0.05 was considered to be statistically significant. Sensitivity (pEC₅₀)
136 to ACh and NS309 was determined in GraphPad Prism (version 7) using nonlinear
137 regression (variable slope with four parameters; constrains: TOP: 100, BOTTOM, 0).

138

139 **Results**

140 **Comparable body weight after 3 months of a high fat diet regimen**

141 The average age at euthanization was similar for all four mice groups (28 ± 1 g for
142 lean/saline, 28 ± 1 g for obese/saline, 28 ± 1 g for lean/rhTrx, and 28 ± 2 g for
143 obese/rhTrx). Body weight progressively increased during the 3-month high fat regimen
144 or normal diet in both saline-infused and rhTrx-injected mice (Figure 1A). The body weight
145 gain was roughly 15 g for mice placed on a high fat diet for 13 weeks (Figure 1B). Tail
146 vein injection of rhTrx did not result in a statistically significantly different body weight gain
147 compared to saline injection (Figure 1B).

148

149 **Tail vein injection of rhTrx prevents high fat-induced inward remodeling of small** 150 **mesenteric arteries**

151 Second-order branches of the superior mesenteric artery (MA2) from all 4 experimental
152 groups were mounted on an isometric wire-myograph system. Following incubation for
153 30 min, arteries were stretched as described in the Methods section. Optimal diameters
154 from MA2 from obese/saline mice were statistically significantly reduced compared to
155 their lean counterparts (Figure 1C; 168 ± 5 μm versus 184 ± 5 μm , respectively). Infusion
156 of rhTrx prevented this inward remodeling after a high-fat diet, since optimal diameters
157 were comparable for both lean and obese mice that were given rhTrx (Figure 1C; $183 \pm$
158 5 μm versus 182 ± 4 μm , respectively). Active wall tension (in mN/mm) in response to a
159 depolarizing KRB solution containing 60 mM KCl were comparable in MA2 for all
160 experimental mice groups (Figure 1D). Coronary artery optimal diameter (Figure 1E) and

161 active wall tension (Figure 1F) were similar for the four experimental mice groups,
162 although wall tensions tended to be larger in the obese/rhTrx group (Figure 1F). Femoral
163 artery optimal diameter tended to be smaller in the obese/saline group compared to the
164 other three groups (Figure 1G), but active wall tension were statistically significantly
165 reduced compared to the other three groups (Figure 1H).

166

167 **Contractile responses are comparable for all experimental groups**

168 Phenylephrine contracted MA2 in a concentration-dependent manner (Figure 2A).
169 Normalized (as percentage of 60 mM KCl) concentration-response curves (CRC) showed
170 no significant differences in both sensitivity (pEC_{50}) and maximum contraction (E_{max}) for
171 PHE in all groups (Figure 1). Serotonin (5-HT) contracted coronary and femoral arteries
172 in a concentration-dependent manner (Figure 2). Similarly to MA2, no significant
173 differences in pEC_{50} and E_{max} were observed between the experimental groups for both
174 artery types.

175

176 **Acetylcholine-induced relaxing responses are impaired in MA2 and femoral** 177 **arteries from obese/saline mice, but not in obese/rhTrx mice**

178 Acetylcholine relaxed MA2, coronary and femoral arteries in a concentration-dependent
179 manner (Figure 3A – 3C). This relaxation was diminished in MA2 and femoral arteries,
180 but not coronary arteries, derived from obese mice injected with saline. In MA2, pEC_{50}
181 was decreased 10-fold in obese/saline compared to lean/saline (5.45 ± 0.08 versus 6.55
182 ± 0.05 ; $P < 0.05$; Figure 3A). E_{max} was significantly diminished in obese/saline compared

183 to lean/saline ($58 \pm 6\%$ versus $85 \pm 3\%$; $P < 0.05$; Figure 3A). ACh-induced relaxations
184 were comparable in MA2 between lean/saline and lean/rhTrx mice (Figure 3A). Strikingly,
185 tail vein infusion of rhTrx completely prevented the high fat-induced ACh-induced
186 impairment, with pEC_{50} and E_{max} values similar to lean/saline values (6.25 ± 0.08 and 75
187 $\pm 7\%$, respectively; Figure 3A). A similar trend was observed in femoral arteries, but the
188 differences were not as pronounced as in MA2 (Figure 3C). ACh-induced relaxations in
189 coronary arteries were comparable for all experimental groups (Figure 3B). The observed
190 impairments in ACh-induced relaxations were endothelium-dependent since relaxing
191 responses to sodium nitroprusside, a NO donor with endothelium-independent relaxing
192 properties, were not statistically significant between all groups for MA2, coronary and
193 femoral arteries (Figure 3D – 3F).

194

195 **NO release is diminished in MA2 from obese/saline mice, but preserved in**
196 **obese/rhTrx**

197 The suppressing role of endothelial derived NO in PHE-induced contractions was
198 analyzed by comparing CRCs to PHE in the absence and presence of L-NAME. Figure
199 4A to 4D shows contractions to PHE for MA2 derived from the four groups. The area
200 between the curves is highlighted in light blue. In a similar fashion, the role of NO in ACh-
201 mediated relaxing responses was assessed. Figure 4E to 4H shows ACh-induced
202 relaxing responses in the absence and presence of L-NAME with the light blue areas as
203 area between the curves. The area under/above the curves (AUC for PHE or AAC for
204 ACh) and the arbitrary units of the areas between the curves are depicted in Figure 4I to
205 4L. The surface area of the light blue areas are smaller for MA2 from obese/saline mice

206 (Figure 4G, 4E, and 4J) compared to the other three groups, highlighting a diminished
207 functional role of NO in vasomotor responses. More importantly, the role of NO in these
208 responses is completely protected by tail vein injections of rhTrx (Figure 4D, 4H, and 4L).

209

210 **EDH relaxing responses are diminished in obese/saline, but preserved in**
211 **obese/rhTrx**

212 The contribution of endothelial K_{Ca} channels on the EDH relaxing response was
213 determined via two pharmacological approaches. The first approach assesses
214 differences between CRCs to ACh and NS309 in the absence and presence of the two
215 endothelial K_{Ca} channel blockers TRAM-34 and UCL-1684. Figure 5A to 5D shows the
216 contribution of endothelial K_{Ca} channels that were activated indirectly via ACh-induced
217 signaling for the four groups. The yellow highlighted areas show the ABC and are an
218 indication of the magnitude of endothelial K_{Ca} involvement in response to ACh. The middle
219 panel of graphs (Figure 5E to 5H) depict the contribution of these K_{Ca} channels after direct
220 opening by NS309, with the magnitude of the EDH response highlighted in yellow. The
221 areas under the curve (AUC) for all graphs are summarized in the bar graphs (Figure 5I
222 to 5L). The extent of the yellow highlighted areas are shown as differences between bar
223 heights. No significant difference between the bar graphs was observed for obese/saline
224 mice, indicating blunted EDH response in these vessels (Figure 5J). Tail vein injections
225 of rhTrx completely prevented the high fat-induced reduction in the EDH response (Figure
226 5L).

227 Historically, the EDH-mediated response is analyzed in the presence of L-NAME and
228 indomethacin. Figure 6A shows that ACh-induced EDH responses were smallest in MA2
229 from obese/saline mice. AAC values were significantly reduced in MA2 from obese/saline
230 compared to the other groups (Figure 6B). Sensitivity for ACh was significantly lower in
231 MA2 from obese/saline mice compared to the other groups (Figure 6C). NS309-induced
232 relaxing responses were reduced in MA2 from obese/saline mice compared to the other
233 groups (Figure 6D). AAC (Figure 6E) and sensitivity (Figure 6F) for NS309 were
234 significantly decreased in obese/saline compared to the other groups. Again, tail vein
235 injections of rhTrx completely prevented the high fat-induced blunted EDH response.

236

237 **Discussion**

238 The present isometric myograph functional data support the hypothesis that tail vein
239 injections of human recombinant thioredoxin completely protects against high fat-induced
240 endothelial dysfunction in small mesenteric and femoral arteries. In small mesenteric
241 arteries this protection is characterized by an increased NO and EDH relaxing response,
242 the latter via enhanced endothelial K_{Ca} channel opening.

243 Obesity is a major risk factor for the development of cardiovascular and metabolic
244 complications such as hypertension and type 2 diabetes [13, 14]. This mouse strain is
245 well suited because of its high sensitivity for obesity and type 2 diabetes in response to a
246 high fat diet [15]. The objective of this study was not to assess plasma triglycerides and
247 cholesterol levels, weigh subcutaneous and epididymal fat mass in order to confirm a
248 metabolic syndrome. Here an obesity-induced diet (42% kcal from fat) was used to elicit
249 an endothelial dysfunction in small arteries derived from C57Bl6/J mice. This was
250 successful since small mesenteric and skeletal femoral arteries isolated from saline-
251 injected obese mice presented classical signs of endothelial dysfunction: blunted ACh-
252 induced relaxing responses. Judged from the comparable body weight gain during the 13
253 week high fat diet for saline- or rhTrx-injected obese mice, the injection of rhTrx did not
254 have a significant impact on body mass gain. A dose of 25 mg/kg of rhTrx was chosen to
255 inject via the tail vein. This dose was comparable to the dose used before, which resulted
256 in detectable plasma levels and a blood pressure lowering effect in aged hypertensive
257 mice [9].

258 Resistance arteries play a crucial role in blood pressure regulation and local tissue
259 perfusion, as well as their capacity to adapt to hemodynamic changes (e.g. pressure,

260 stretch and flow) [16, 17]. The optimal diameters of second-order mesenteric arteries
261 (MA2) derived from obese/saline mice were significantly smaller than their lean
262 counterparts, suggesting inward remodeling during obesity. Inward remodeling of small
263 arteries has been observed in patients with essential hypertension [18], in cerebral
264 arteries of obese rats [19], and in mesenteric arteries that underwent surgical blood flow
265 cessation [20]. The optimal diameters were determined via horizontal stretching of
266 isolated arteries in the wire-myograph. No pressure-myography and morphological
267 analysis were performed to prove that the observed smaller optimal diameters were in
268 fact the result of anatomical structural adaptations to obesity. Coronary and femoral
269 arteries had similar optimal diameters for the four experimental groups, which suggests
270 a regio heterogeneous effect.

271 Contractile responses in the absence of any inhibitors were unaltered irrespective
272 of diet and treatment in MA2, coronary and femoral arteries. However, endothelium-
273 dependent ACh-induced relaxing responses were impaired in MA2 and femoral arteries
274 derived from obese/saline compared to the three counterparts. Endothelium-independent
275 relaxing responses by the NO donor sodium nitroprusside were comparable for all groups
276 and artery types. These observations demonstrate that the observed differences in ACh-
277 induced responses were manifested at the level of the endothelium.

278 The mesenteric arterial bed is prone to high fat-induced impairment in
279 endothelium-dependent relaxation, probably due to the close proximity of intestinal
280 absorption of fatty acids. The small mesenteric artery is a preferred choice of resistance-
281 sized artery for the vascular biologist due to its abundance and relative ease of dissection.
282 Hence, endothelial dysfunction in response to obesity has been shown in murine small

283 mesenteric arteries [21-25], but some studies did not observe an impairment in ACh-
284 induced relaxation [26-28]. Similarly, a high-fat diet has been shown to result in either
285 preserved endothelial function [29, 30] or impaired endothelial function in murine coronary
286 arteries [31, 32]. Similar to this study, impaired ACh-induced relaxing responses in
287 femoral arteries were observed in C57Bl6/J mice that received a high fat diet [30].

288 A pharmacological approach was used to assess the role of NO and the
289 endothelium-dependent hyperpolarizing (EDH) relaxing response in MA2. In general,
290 indomethacin is used in *ex vivo* vascular reactivity studies to block cyclo-oxygenases that
291 produce vasoactive prostaglandins. Here, all MA2 were treated with indomethacin to rule
292 out any contribution of vasoactive prostaglandins. In the present study, the main
293 mechanism of endothelium-dependent relaxation in the murine small mesenteric artery
294 was via NO release and EDH, which is in agreement with other studies [10, 33, 34]. In
295 obese and saline-injected mice, both the NO- and EDH-dependent relaxation in MA2
296 were significantly impaired compared to lean and saline-injected mice. This observation
297 is congruent with other studies using a high fat diet and small mesenteric arteries in the
298 myograph [21, 22, 35]. EDH responses were assessed with both ACh (indirectly) and
299 NS309 (directly), a non-selective endothelial IK_{Ca} and SK_{Ca} channel opener [12]. ACh
300 increases intracellular Ca^{2+} ions in endothelial cells that activate endothelial K_{Ca} channels,
301 whereas NS309 is an opener of these K_{Ca} channels. In murine small mesenteric arteries,
302 the IK_{Ca} (or $IK1$) channel contributes mainly to ACh-stimulated Ca^{2+} dynamics [36] and
303 genetic knockdown of $IK1$ reduces ACh-induced EDH response in murine mesenteric
304 arteries [37, 38]. In agreement with these observations, the NS309-induced EDH
305 response was inhibited by TRAM-34 and not by UCL-1684 (data not shown), confirming

306 the importance of the IK_{Ca} channel in this species and artery type. The IK_{Ca} channel can
307 be oxidized by hydrogen peroxide (H_2O_2) and other chemical cysteine thiol oxidizers, like
308 5,5'-dithio-bis (2-nitrobenzoic acid) (DTNB or Ellman's reagent) or [(O-
309 carboxyphenyl)thio]ethyl mercury sodium salt (thimerosal), to inhibit IK_{Ca} channel activity
310 in bovine aortic endothelial cells [39]. Thiol reducing agents like dithiotreitol or reduced
311 glutathione were able to restore the IK_{Ca} channel activity. *In vivo*, the IK_{Ca} channel can be
312 inactivated by oxidative stress factors like obesity and hyperhomocysteinemia [40, 41].
313 Interestingly, the nonluminal S6 region of the IK_{Ca} channel protein, which is crucial in
314 pore-forming, contains two adjacent cysteine residues (Cys276 and -277), which have
315 the potential to become subject to post-translational thiol modification [42]. The above
316 observations suggest redox modulation of the IK_{Ca} channel with an important modulatory
317 role for thioredoxin. Using transgenic mice overexpressing human thioredoxin-1 (Trx-Tg),
318 an enhanced EDH response was observed in MA2 compared to non-transgenic mice [10].
319 Furthermore, endothelial NO release was enhanced in aortae of Trx-Tg mice [9]. These
320 observations prompted the idea of exogenously administering rhTrx in mice in an effort
321 to study whether rhTrx could protect against high fat-induced endothelial dysfunction.

322 Tail vein injection of rhTrx completely protected endothelium-dependent relaxing
323 responses in MA2 against a high fat diet, via an increased NO release and enhanced
324 EDH response. The latter was mediated via endothelial K_{Ca} channel activation. This
325 observation strongly suggests that redox modulation of cysteine thiol groups on proteins
326 regulates the release of endothelial-derived NO and EDH. Trx is also an antioxidant,
327 because it scavenges hydroxyl radicals [43]. It could therefore be argued that the
328 beneficial effects observed by rhTrx are attributed to its antioxidant activity. However,

329 dominant-negative Trx mice, which express a mutant Trx without the catalytic two
330 cysteine residues, but still possess radical scavenging properties, display blunted EDH-
331 mediated relaxing responses in MA2 [10]. Whether Trx directly modulates K_{Ca} channel
332 activity needs to be elucidated. A novel IK_{Ca} selective positive-gating modulator, SKA-31
333 [44], potentiated the EDH response in porcine coronary arteries, suggesting the important
334 role of the IK_{Ca} channel in this artery [45]. Hence, Trx may have beneficial protective
335 effects on coronary blood flow during conditions that reduce expression of endothelial K_{Ca}
336 channels, such as diabetes [46-48] and hypertension [49-51].

337 In conclusion, tail vein injection of rhTrx completely protected obese mice from
338 high fat-induced endothelial dysfunction. In addition, compared to lean/saline-injected
339 mice, NO and EDH-mediated responses were enhanced in MA2 from obese/rhTrx-
340 injected mice. These vasoprotective actions of Trx may provide a promising therapeutic
341 potential in the combat of oxidative stress-linked pathologies.

342

343 **Acknowledgement**

344 Funding for this study was supported by a New Investigator Award (2019) from the
345 American Association of Colleges of Pharmacy.

346

347

348 **Figure Legends**

349 **Figure 1.** Body weight (in g) increases during the 3-month diet regimens (**A**) and body
350 weight at the time of euthanization (**B**) for the four experimental groups. Optimal
351 diameters (in μm) for MA2 (**C**), coronary (**E**), and femoral arteries (**G**) obtained via
352 isometric myography. Active wall tension (in mN/mm) in response to 60 mM KCl in KRB
353 for MA2 (**D**), coronary (**F**), and femoral arteries (**H**). Values are expressed in mean \pm
354 S.E.M. * $P < 0.05$ obese/saline versus lean/saline; # $P < 0.05$ obese/saline versus
355 obese/rhTrx.

356 **Figure 2.** Contractile responses to the α_1 -adrenergic agonist phenylephrine (PHE; 0.01
357 – 30 μM) in MA2 (**A**), coronary (**B**) and femoral arteries (**C**) for the four experimental
358 groups. Values are expressed in mean \pm S.E.M.

359 **Figure 3.** Endothelium-dependent ACh-induced relaxation in MA2 (**A**), coronary (**B**) and
360 femoral arteries (**C**) for the four experimental groups. Endothelium-independent
361 relaxations to the NO donor sodium nitroprusside (SNP) in MA2 (**D**), coronary (**E**) and
362 femoral arteries (**F**) for the four experimental groups. Values are expressed in mean \pm
363 S.E.M. * $P < 0.05$ obese/saline versus the three other groups.

364 **Figure 4.** Contribution of NO in vasomotor responses. Contractile responses to the α_1 -
365 adrenergic agonist phenylephrine (PHE; 0.01 – 30 μM) in MA2 in the absence (CON,
366 open circles) and presence of L-NAME (100 μM , closes circles) for lean/saline (**A**),
367 obese/saline (**B**), lean/rhTrx (**C**) and obese/rhTrx mice (**D**). Endothelium-dependent ACh-
368 induced relaxation in MA2 in the absence (CON) and presence L-NAME (100 μM) for
369 lean/saline (**E**), obese/saline (**F**), lean/rhTrx (**G**) and obese/rhTrx mice (**H**). Hghlighted

370 blue areas represent the contribution of NO. Calculated area under the curve (AUC) for
371 PHE-induced contractions (black) and calculated area above the curve (AAC) for ACh-
372 induced (purple) responses for lean/saline (**I**), obese/saline (**J**), lean/rhTrx (**K**) and
373 obese/rhTrx mice (**L**). Differences in AAC or AUC (Δ) are shown. All arteries were
374 incubated with indomethacin (10 μ M). Values are expressed in mean \pm S.E.M. * $P < 0.05$,
375 # $P < 0.001$, NS is not significant.

376 **Figure 5.** Contribution of EDH. Endothelium-dependent ACh-induced (**A** to **D**) and
377 NS309-induced (**E** to **H**) relaxing responses in MA2 in the absence (CON, open symbols)
378 and the presence of TRAM-34 (10 μ M) + UCL-1684 (1 μ M) (closed circles) for lean/saline
379 (**A** and **E**), obese/saline (**B** and **F**), lean/rhTrx (**C** and **G**), and obese/rhTrx (**D** and **H**). Light
380 blue areas represents the contribution of EDH via endothelial K_{Ca} channel activation.
381 Calculated area under the curve (AUC) for ACh-induced responses (black) and NS309-
382 induced responses (green) for lean/saline (**I**), obese/saline (**J**), lean/rhTrx (**K**) and
383 obese/rhTrx mice (**L**). Differences in AUC (Δ) are shown. All arteries were incubated with
384 indomethacin (10 μ M). Values are expressed in mean \pm S.E.M. * $P < 0.05$, # $P < 0.001$,
385 NS is not significant.

386 **Figure 6.** Endothelium-dependent ACh-induced (**A** to **C**) and NS309-induced (**D** to **F**)
387 relaxing responses in MA2 in the presence of L-NAME in lean/saline (open black circles
388 or bars), obese/saline (closed black circles or bars), lean/rhTrx (open blue circles or bars),
389 and obese/rhTrx (closed blue circles or bars). Area above the curve are summarized in
390 (**B** and **E**). Sensitivity (pEC_{50}) are summarized in (**C** and **F**). All arteries were incubated
391 with indomethacin (10 μ M). Values are expressed in mean \pm S.E.M. * $P < 0.05$
392 obese/saline versus all other groups.

393 References

- 394 1. Garland CJ, Dora KA. EDH: endothelium-dependent hyperpolarization and microvascular
395 signalling. *Acta Physiol (Oxf)*. 2017;219(1):152-61. Epub 2016/01/12. doi: 10.1111/apha.12649. PubMed
396 PMID: 26752699.
- 397 2. Crane GJ, Gallagher N, Dora KA, Garland CJ. Small- and intermediate-conductance calcium-
398 activated K⁺ channels provide different facets of endothelium-dependent hyperpolarization in rat
399 mesenteric artery. *J Physiol*. 2003;553(Pt 1):183-9. Epub 2003/10/14. doi: 10.1113/jphysiol.2003.051896.
400 PubMed PMID: 14555724; PubMed Central PMCID: PMCPMC2343487.
- 401 3. Coleman HA, Tare M, Parkington HC. Endothelial potassium channels, endothelium-dependent
402 hyperpolarization and the regulation of vascular tone in health and disease. *Clin Exp Pharmacol Physiol*.
403 2004;31(9):641-9. Epub 2004/10/14. doi: 10.1111/j.1440-1681.2004.04053.x. PubMed PMID: 15479173.
- 404 4. Goto K, Ohtsubo T, Kitazono T. Endothelium-Dependent Hyperpolarization (EDH) in Hypertension:
405 The Role of Endothelial Ion Channels. *Int J Mol Sci*. 2018;19(1). Epub 2018/01/25. doi:
406 10.3390/ijms19010315. PubMed PMID: 29361737; PubMed Central PMCID: PMCPMC5796258.
- 407 5. Kanaan GN, Harper ME. Cellular redox dysfunction in the development of cardiovascular diseases.
408 *Biochim Biophys Acta Gen Subj*. 2017;1861(11 Pt A):2822-9. Epub 2017/08/06. doi:
409 10.1016/j.bbagen.2017.07.027. PubMed PMID: 28778485.
- 410 6. Munzel T, Camici GG, Maack C, Bonetti NR, Fuster V, Kovacic JC. Impact of Oxidative Stress on the
411 Heart and Vasculature: Part 2 of a 3-Part Series. *J Am Coll Cardiol*. 2017;70(2):212-29. Epub 2017/07/08.
412 doi: 10.1016/j.jacc.2017.05.035. PubMed PMID: 28683969; PubMed Central PMCID: PMCPMC5663297.
- 413 7. Hanschmann EM, Godoy JR, Berndt C, Hudemann C, Lillig CH. Thioredoxins, glutaredoxins, and
414 peroxiredoxins--molecular mechanisms and health significance: from cofactors to antioxidants to redox
415 signaling. *Antioxid Redox Signal*. 2013;19(13):1539-605. Epub 2013/02/13. doi: 10.1089/ars.2012.4599.
416 PubMed PMID: 23397885; PubMed Central PMCID: PMCPMC3797455.
- 417 8. Holmgren A. Thioredoxin. *Annu Rev Biochem*. 1985;54:237-71. Epub 1985/01/01. doi:
418 10.1146/annurev.bi.54.070185.001321. PubMed PMID: 3896121.
- 419 9. Hilgers RH, Kundumani-Sridharan V, Subramani J, Chen LC, Cuello LG, Rusch NJ, et al. Thioredoxin
420 reverses age-related hypertension by chronically improving vascular redox and restoring eNOS function.
421 *Sci Transl Med*. 2017;9(376). Epub 2017/02/10. doi: 10.1126/scitranslmed.aaf6094. PubMed PMID:
422 28179506; PubMed Central PMCID: PMCPMC5808940.
- 423 10. Hilgers RH, Das KC. Role of in vivo vascular redox in resistance arteries. *Hypertension*.
424 2015;65(1):130-9. Epub 2014/10/15. doi: 10.1161/HYPERTENSIONAHA.114.04473. PubMed PMID:
425 25312439; PubMed Central PMCID: PMCPMC4268237.
- 426 11. Subramani J, Kundumani-Sridharan V, Hilgers RH, Owens C, Das KC. Thioredoxin Uses a GSH-
427 independent Route to Deglutathionylate Endothelial Nitric-oxide Synthase and Protect against Myocardial
428 Infarction. *J Biol Chem*. 2016;291(45):23374-89. Epub 2016/09/03. doi: 10.1074/jbc.M116.745034.
429 PubMed PMID: 27587398; PubMed Central PMCID: PMCPMC5095395.
- 430 12. Strobaek D, Teuber L, Jorgensen TD, Ahring PK, Kjaer K, Hansen RS, et al. Activation of human IK
431 and SK Ca²⁺-activated K⁺ channels by NS309 (6,7-dichloro-1H-indole-2,3-dione 3-oxime). *Biochim*
432 *Biophys Acta*. 2004;1665(1-2):1-5. Epub 2004/10/09. doi: 10.1016/j.bbamem.2004.07.006. PubMed
433 PMID: 15471565.
- 434 13. Li M, Qian M, Xu J. Vascular Endothelial Regulation of Obesity-Associated Insulin Resistance. *Front*
435 *Cardiovasc Med*. 2017;4:51. Epub 2017/08/30. doi: 10.3389/fcvm.2017.00051. PubMed PMID: 28848738;
436 PubMed Central PMCID: PMCPMC5552760.

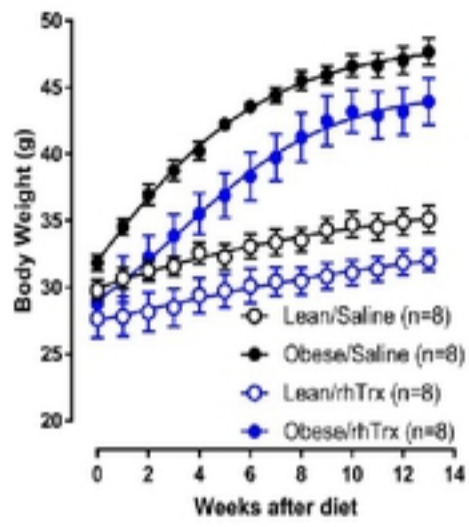
- 437 14. Alpert MA, Omran J, Bostick BP. Effects of Obesity on Cardiovascular Hemodynamics, Cardiac
438 Morphology, and Ventricular Function. *Curr Obes Rep.* 2016;5(4):424-34. Epub 2016/10/17. doi:
439 10.1007/s13679-016-0235-6. PubMed PMID: 27744513.
- 440 15. Collins S, Martin TL, Surwit RS, Robidoux J. Genetic vulnerability to diet-induced obesity in the
441 C57BL/6J mouse: physiological and molecular characteristics. *Physiol Behav.* 2004;81(2):243-8. Epub
442 2004/05/26. doi: 10.1016/j.physbeh.2004.02.006. PubMed PMID: 15159170.
- 443 16. Henrion D. Pressure and flow-dependent tone in resistance arteries. Role of myogenic tone. *Arch
444 Mal Coeur Vaiss.* 2005;98(9):913-21. Epub 2005/10/20. PubMed PMID: 16231579.
- 445 17. De Mey JG, Schiffers PM, Hilgers RH, Sanders MM. Toward functional genomics of flow-induced
446 outward remodeling of resistance arteries. *Am J Physiol Heart Circ Physiol.* 2005;288(3):H1022-7. Epub
447 2005/02/12. doi: 10.1152/ajpheart.00800.2004. PubMed PMID: 15706039.
- 448 18. Schofield I, Malik R, Izzard A, Austin C, Heagerty A. Vascular structural and functional changes in
449 type 2 diabetes mellitus: evidence for the roles of abnormal myogenic responsiveness and dyslipidemia.
450 *Circulation.* 2002;106(24):3037-43. Epub 2002/12/11. PubMed PMID: 12473548.
- 451 19. Deutsch C, Portik-Dobos V, Smith AD, Ergul A, Dorrance AM. Diet-induced obesity causes cerebral
452 vessel remodeling and increases the damage caused by ischemic stroke. *Microvasc Res.* 2009;78(1):100-
453 6. Epub 2009/04/21. doi: 10.1016/j.mvr.2009.04.004. PubMed PMID: 19374911; PubMed Central PMCID:
454 PMC3959658.
- 455 20. Pourageaud F, De Mey JG. Structural properties of rat mesenteric small arteries after 4-wk
456 exposure to elevated or reduced blood flow. *Am J Physiol.* 1997;273(4 Pt 2):H1699-706. Epub 1997/11/15.
457 PubMed PMID: 9362233.
- 458 21. Aoqui C, Chmielewski S, Scherer E, Eissler R, Sollinger D, Heid I, et al. Microvascular dysfunction in
459 the course of metabolic syndrome induced by high-fat diet. *Cardiovasc Diabetol.* 2014;13:31. Epub
460 2014/02/05. doi: 10.1186/1475-2840-13-31. PubMed PMID: 24490784; PubMed Central PMCID:
461 PMC3916304.
- 462 22. Tian XY, Wong WT, Xu A, Lu Y, Zhang Y, Wang L, et al. Uncoupling protein-2 protects endothelial
463 function in diet-induced obese mice. *Circ Res.* 2012;110(9):1211-6. Epub 2012/03/31. doi:
464 10.1161/CIRCRESAHA.111.262170. PubMed PMID: 22461387.
- 465 23. Dunn SM, Hilgers RH, Das KC. Decreased EDHF-mediated relaxation is a major mechanism in
466 endothelial dysfunction in resistance arteries in aged mice on prolonged high-fat sucrose diet. *Physiol Rep.*
467 2017;5(23). Epub 2017/12/08. doi: 10.14814/phy2.13502. PubMed PMID: 29212858; PubMed Central
468 PMCID: PMC5727270.
- 469 24. Wang H, Luo W, Wang J, Guo C, Wang X, Wolffe SL, et al. Obesity-induced endothelial dysfunction
470 is prevented by deficiency of P-selectin glycoprotein ligand-1. *Diabetes.* 2012;61(12):3219-27. Epub
471 2012/08/15. doi: 10.2337/db12-0162. PubMed PMID: 22891216; PubMed Central PMCID:
472 PMC3501858.
- 473 25. Gil-Ortega M, Condezo-Hoyos L, Garcia-Prieto CF, Arribas SM, Gonzalez MC, Aranguiz I, et al.
474 Imbalance between pro and anti-oxidant mechanisms in perivascular adipose tissue aggravates long-term
475 high-fat diet-derived endothelial dysfunction. *PLoS One.* 2014;9(4):e95312. Epub 2014/04/25. doi:
476 10.1371/journal.pone.0095312. PubMed PMID: 24760053; PubMed Central PMCID: PMC3997398.
- 477 26. Eichhorn B, Muller G, Leuner A, Sawamura T, Ravens U, Morawietz H. Impaired vascular function
478 in small resistance arteries of LOX-1 overexpressing mice on high-fat diet. *Cardiovasc Res.* 2009;82(3):493-
479 502. Epub 2009/03/18. doi: 10.1093/cvr/cvp089. PubMed PMID: 19289377.
- 480 27. Ellis A, Cheng ZJ, Li Y, Jiang YF, Yang J, Pannirselvam M, et al. Effects of a Western diet versus high
481 glucose on endothelium-dependent relaxation in murine micro- and macro-vasculature. *Eur J Pharmacol.*
482 2008;601(1-3):111-7. Epub 2008/11/11. doi: 10.1016/j.ejphar.2008.10.042. PubMed PMID: 18996368.
- 483 28. Soares AG, de Carvalho MHC, Akamine E. Obesity Induces Artery-Specific Alterations: Evaluation
484 of Vascular Function and Inflammatory and Smooth Muscle Phenotypic Markers. *Biomed Res Int.*

- 485 2017;2017:5038602. Epub 2017/05/04. doi: 10.1155/2017/5038602. PubMed PMID: 28466012; PubMed
486 Central PMCID: PMCPMC5390568.
- 487 29. Feher A, Rutkai I, Beleznai T, Ungvari Z, Csiszar A, Edes I, et al. Caveolin-1 limits the contribution
488 of BK(Ca) channel to EDHF-mediated arteriolar dilation: implications in diet-induced obesity. *Cardiovasc*
489 *Res.* 2010;87(4):732-9. Epub 2010/03/20. doi: 10.1093/cvr/cvq088. PubMed PMID: 20299334; PubMed
490 Central PMCID: PMCPMC2920808.
- 491 30. Bender SB, Castorena-Gonzalez JA, Garro M, Reyes-Aldasoro CC, Sowers JR, DeMarco VG, et al.
492 Regional variation in arterial stiffening and dysfunction in Western diet-induced obesity. *Am J Physiol*
493 *Heart Circ Physiol.* 2015;309(4):H574-82. Epub 2015/06/21. doi: 10.1152/ajpheart.00155.2015. PubMed
494 PMID: 26092984; PubMed Central PMCID: PMCPMC4537938.
- 495 31. Dou H, Feher A, Davila AC, Romero MJ, Patel VS, Kamath VM, et al. Role of Adipose Tissue
496 Endothelial ADAM17 in Age-Related Coronary Microvascular Dysfunction. *Arterioscler Thromb Vasc Biol.*
497 2017;37(6):1180-93. Epub 2017/05/06. doi: 10.1161/ATVBAHA.117.309430. PubMed PMID: 28473444;
498 PubMed Central PMCID: PMCPMC5484536.
- 499 32. Gamez-Mendez AM, Vargas-Robles H, Rios A, Escalante B. Oxidative Stress-Dependent Coronary
500 Endothelial Dysfunction in Obese Mice. *PLoS One.* 2015;10(9):e0138609. Epub 2015/09/19. doi:
501 10.1371/journal.pone.0138609. PubMed PMID: 26381906; PubMed Central PMCID: PMCPMC4575160.
- 502 33. Dora KA, Sandow SL, Gallagher NT, Takano H, Rummery NM, Hill CE, et al. Myoendothelial gap
503 junctions may provide the pathway for EDHF in mouse mesenteric artery. *J Vasc Res.* 2003;40(5):480-90.
504 Epub 2003/10/30. doi: 10.1159/000074549. PubMed PMID: 14583659.
- 505 34. Godo S, Sawada A, Saito H, Ikeda S, Enkhjargal B, Suzuki K, et al. Disruption of Physiological Balance
506 Between Nitric Oxide and Endothelium-Dependent Hyperpolarization Impairs Cardiovascular
507 Homeostasis in Mice. *Arterioscler Thromb Vasc Biol.* 2016;36(1):97-107. Epub 2015/11/07. doi:
508 10.1161/ATVBAHA.115.306499. PubMed PMID: 26543099.
- 509 35. Brondum E, Kold-Petersen H, Simonsen U, Aalkjaer C. NS309 restores EDHF-type relaxation in
510 mesenteric small arteries from type 2 diabetic ZDF rats. *Br J Pharmacol.* 2010;159(1):154-65. Epub
511 2009/12/18. doi: 10.1111/j.1476-5381.2009.00525.x. PubMed PMID: 20015296; PubMed Central PMCID:
512 PMCPMC2823361.
- 513 36. Qian X, Francis M, Kohler R, Solodushko V, Lin M, Taylor MS. Positive feedback regulation of
514 agonist-stimulated endothelial Ca²⁺ dynamics by KCa_{3.1} channels in mouse mesenteric arteries.
515 *Arterioscler Thromb Vasc Biol.* 2014;34(1):127-35. Epub 2013/11/02. doi: 10.1161/ATVBAHA.113.302506.
516 PubMed PMID: 24177326; PubMed Central PMCID: PMCPMC4181598.
- 517 37. Braehler S, Kaistha A, Schmidt VJ, Wolfle SE, Busch C, Kaistha BP, et al. Genetic deficit of SK3 and
518 IK1 channels disrupts the endothelium-derived hyperpolarizing factor vasodilator pathway and causes
519 hypertension. *Circulation.* 2009;119(17):2323-32. Epub 2009/04/22. doi:
520 10.1161/CIRCULATIONAHA.108.846634. PubMed PMID: 19380617.
- 521 38. Si H, Heyken WT, Wolfle SE, Tysiac M, Schubert R, Grgic I, et al. Impaired endothelium-derived
522 hyperpolarizing factor-mediated dilations and increased blood pressure in mice deficient of the
523 intermediate-conductance Ca²⁺-activated K⁺ channel. *Circ Res.* 2006;99(5):537-44. Epub 2006/07/29.
524 doi: 10.1161/01.RES.0000238377.08219.0c. PubMed PMID: 16873714.
- 525 39. Cai S, Sauve R. Effects of thiol-modifying agents on a K(Ca²⁺) channel of intermediate conductance
526 in bovine aortic endothelial cells. *J Membr Biol.* 1997;158(2):147-58. Epub 1997/07/15. PubMed PMID:
527 9230092.
- 528 40. Zhao L, Wang Y, Ma X, Wang Y, Deng X. Oxidative stress impairs IKCa- and SKCa-mediated
529 vasodilatation in mesenteric arteries from diabetic rats. *Nan Fang Yi Ke Da Xue Xue Bao.* 2013;33(7):939-
530 44. Epub 2013/07/31. PubMed PMID: 23895829.
- 531 41. Cheng Z, Jiang X, Kruger WD, Pratico D, Gupta S, Mallilankaraman K, et al. Hyperhomocysteinemia
532 impairs endothelium-derived hyperpolarizing factor-mediated vasorelaxation in transgenic cystathionine

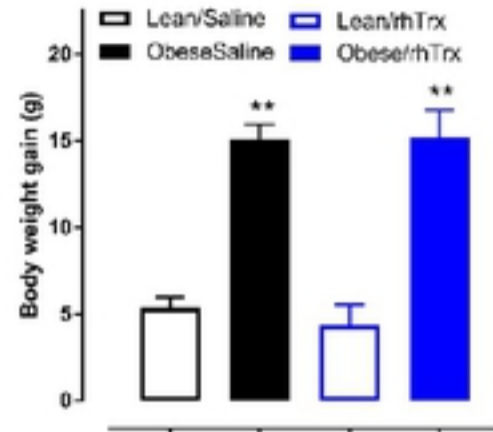
- 533 beta synthase-deficient mice. *Blood*. 2011;118(7):1998-2006. Epub 2011/06/10. doi: 10.1182/blood-
534 2011-01-333310. PubMed PMID: 21653942; PubMed Central PMCID: PMC3158725.
- 535 42. Klein H, Garneau L, Banderali U, Simoes M, Parent L, Sauve R. Structural determinants of the
536 closed KCa3.1 channel pore in relation to channel gating: results from a substituted cysteine accessibility
537 analysis. *J Gen Physiol*. 2007;129(4):299-315. Epub 2007/03/14. doi: 10.1085/jgp.200609726. PubMed
538 PMID: 17353352; PubMed Central PMCID: PMC2151617.
- 539 43. Das KC, Das CK. Thioredoxin, a singlet oxygen quencher and hydroxyl radical scavenger: redox
540 independent functions. *Biochem Biophys Res Commun*. 2000;277(2):443-7. Epub 2000/10/18. doi:
541 10.1006/bbrc.2000.3689. PubMed PMID: 11032742.
- 542 44. Sankaranarayanan A, Raman G, Busch C, Schultz T, Zimin PI, Hoyer J, et al. Naphtho[1,2-d]thiazol-
543 2-ylamine (SKA-31), a new activator of KCa2 and KCa3.1 potassium channels, potentiates the
544 endothelium-derived hyperpolarizing factor response and lowers blood pressure. *Mol Pharmacol*.
545 2009;75(2):281-95. Epub 2008/10/29. doi: 10.1124/mol.108.051425. PubMed PMID: 18955585; PubMed
546 Central PMCID: PMC2635097.
- 547 45. Oliván-Viguera A, Valero MS, Pinilla E, Amor S, García-Villalón AL, Coleman N, et al. Vascular
548 Reactivity Profile of Novel KCa 3.1-Selective Positive-Gating Modulators in the Coronary Vascular Bed.
549 *Basic Clin Pharmacol Toxicol*. 2016;119(2):184-92. Epub 2016/01/29. doi: 10.1111/bcpt.12560. PubMed
550 PMID: 26821335; PubMed Central PMCID: PMC5720859.
- 551 46. Burnham MP, Johnson IT, Weston AH. Impaired small-conductance Ca²⁺-activated K⁺ channel-
552 dependent EDHF responses in Type II diabetic ZDF rats. *Br J Pharmacol*. 2006;148(4):434-41. Epub
553 2006/05/10. doi: 10.1038/sj.bjp.0706748. PubMed PMID: 16682967; PubMed Central PMCID:
554 PMC1751791.
- 555 47. Liu Y, Cole V, Lawandy I, Ehsan A, Sellke FW, Feng J. Decreased coronary arteriolar response to
556 KCa channel opener after cardioplegic arrest in diabetic patients. *Mol Cell Biochem*. 2018;445(1-2):187-
557 94. Epub 2018/01/07. doi: 10.1007/s11010-017-3264-x. PubMed PMID: 29305679; PubMed Central
558 PMCID: PMC6033646.
- 559 48. Weston AH, Absi M, Harno E, Geraghty AR, Ward DT, Ruat M, et al. The expression and function
560 of Ca(2+)-sensing receptors in rat mesenteric artery; comparative studies using a model of type II diabetes.
561 *Br J Pharmacol*. 2008;154(3):652-62. Epub 2008/04/17. doi: 10.1038/bjp.2008.108. PubMed PMID:
562 18414396; PubMed Central PMCID: PMC2439515.
- 563 49. Gschwend S, Henning RH, de Zeeuw D, Buikema H. Coronary myogenic constriction antagonizes
564 EDHF-mediated dilation: role of KCa channels. *Hypertension*. 2003;41(4):912-8. Epub 2003/03/19. doi:
565 10.1161/01.HYP.0000063883.83470.7B. PubMed PMID: 12642510.
- 566 50. Fujii K, Tominaga M, Ohmori S, Kobayashi K, Koga T, Takata Y, et al. Decreased endothelium-
567 dependent hyperpolarization to acetylcholine in smooth muscle of the mesenteric artery of
568 spontaneously hypertensive rats. *Circ Res*. 1992;70(4):660-9. Epub 1992/04/01. PubMed PMID: 1551193.
- 569 51. Hilgers RH, Webb RC. Reduced expression of SKCa and IKCa channel proteins in rat small
570 mesenteric arteries during angiotensin II-induced hypertension. *Am J Physiol Heart Circ Physiol*.
571 2007;292(5):H2275-84. Epub 2007/01/09. doi: 10.1152/ajpheart.00949.2006. PubMed PMID: 17209000.

Figure 1

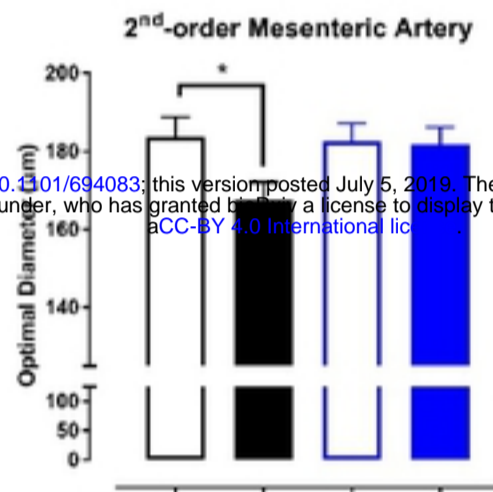
A



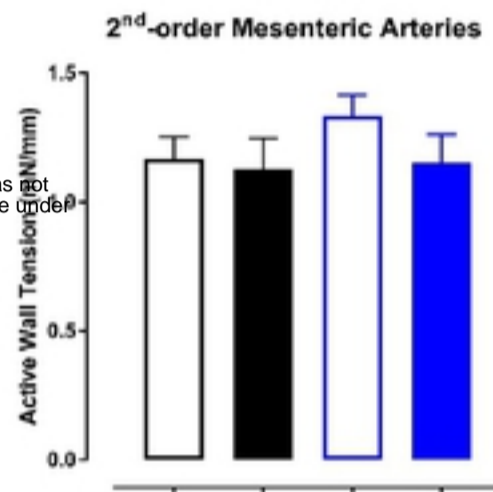
B



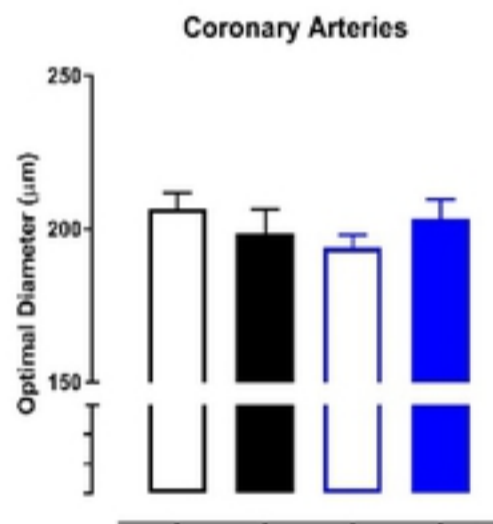
C



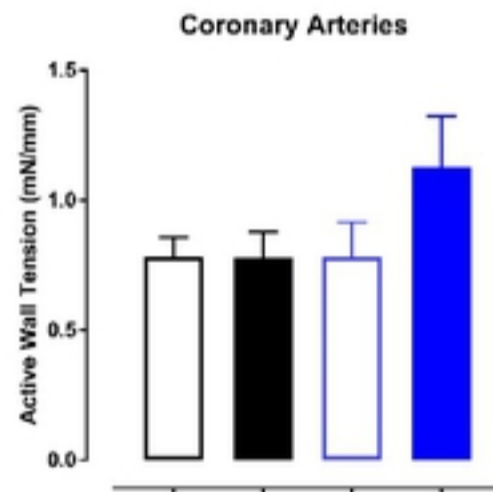
D



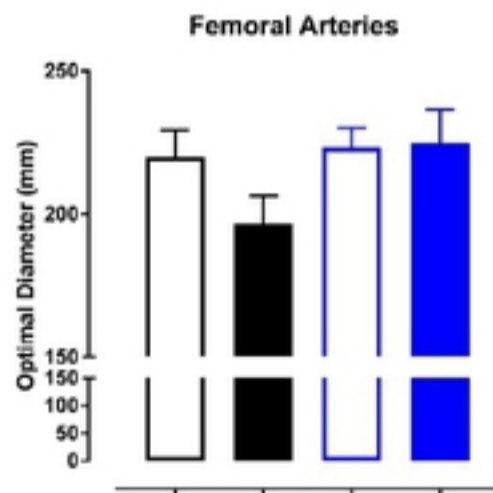
E



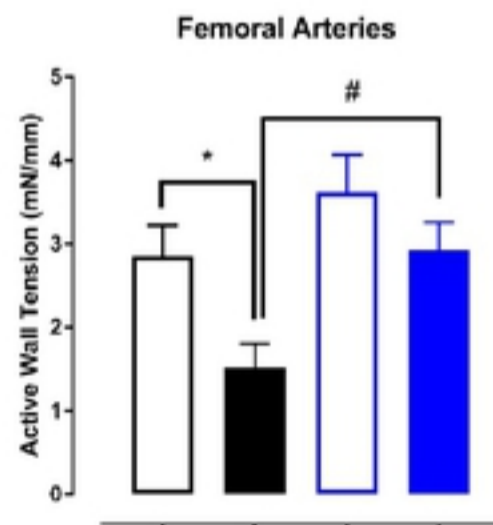
F



G



H



bioRxiv preprint doi: <https://doi.org/10.1101/694083>; this version posted July 5, 2019. The copyright holder for this preprint (which was not certified by peer review) is the author/funder, who has granted bioRxiv a license to display the preprint in perpetuity. It is made available under aCC-BY 4.0 International license.

Figure 2

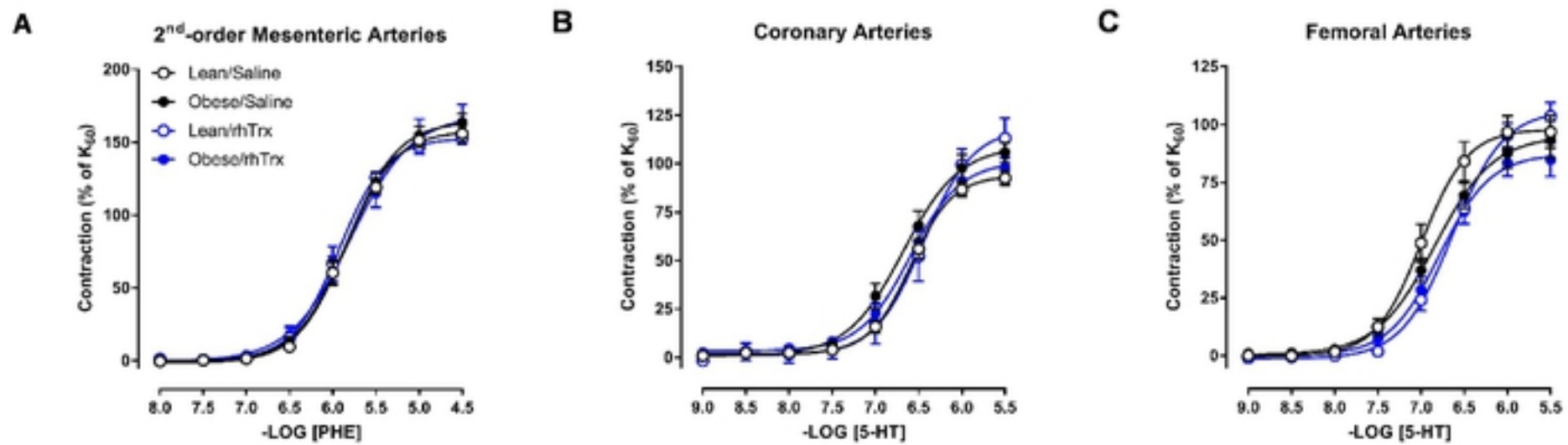


Figure 2

Figure 3

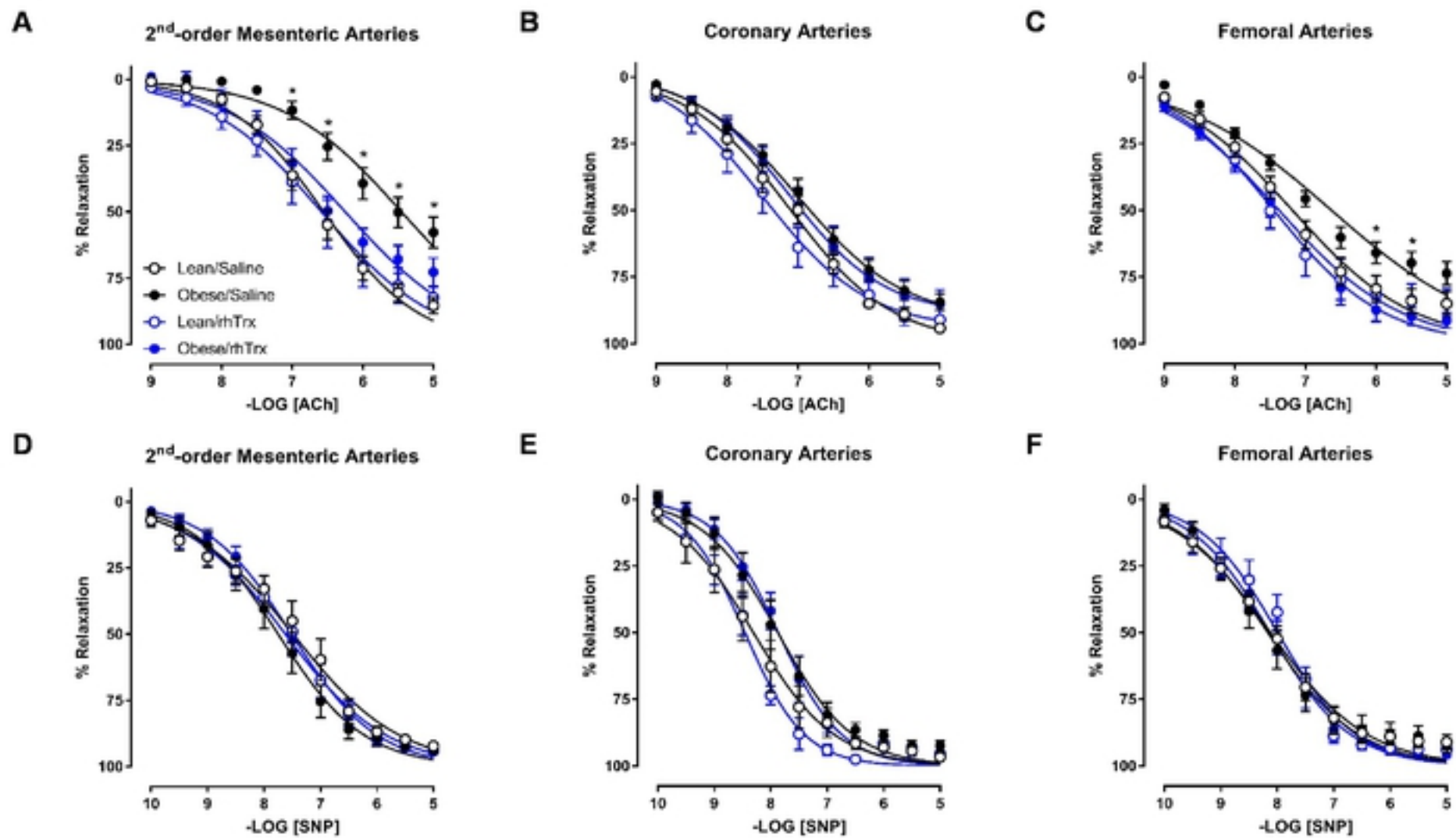


Figure 3

Figure 4



Figure 4

Figure 5

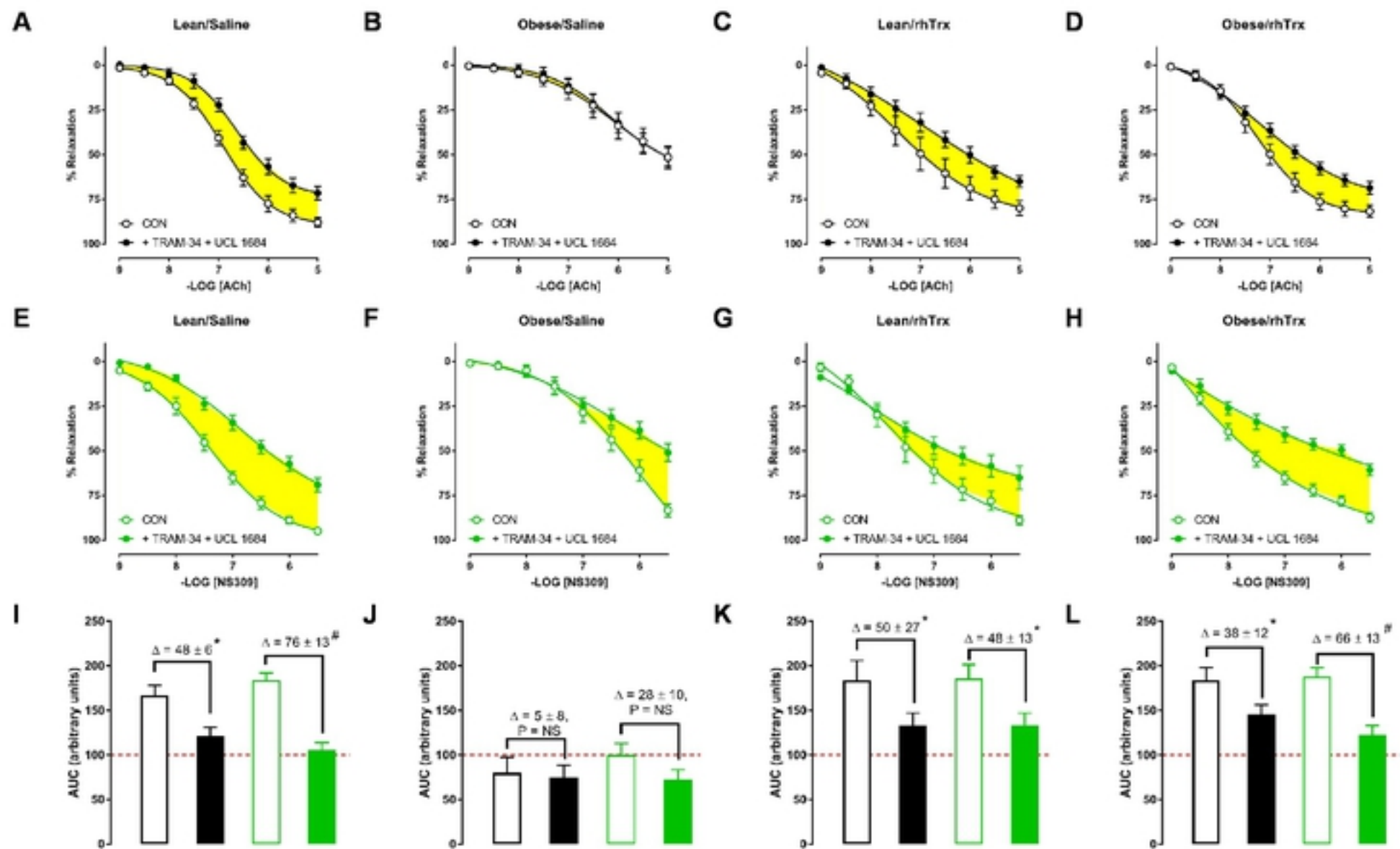


Figure 5

Figure 6

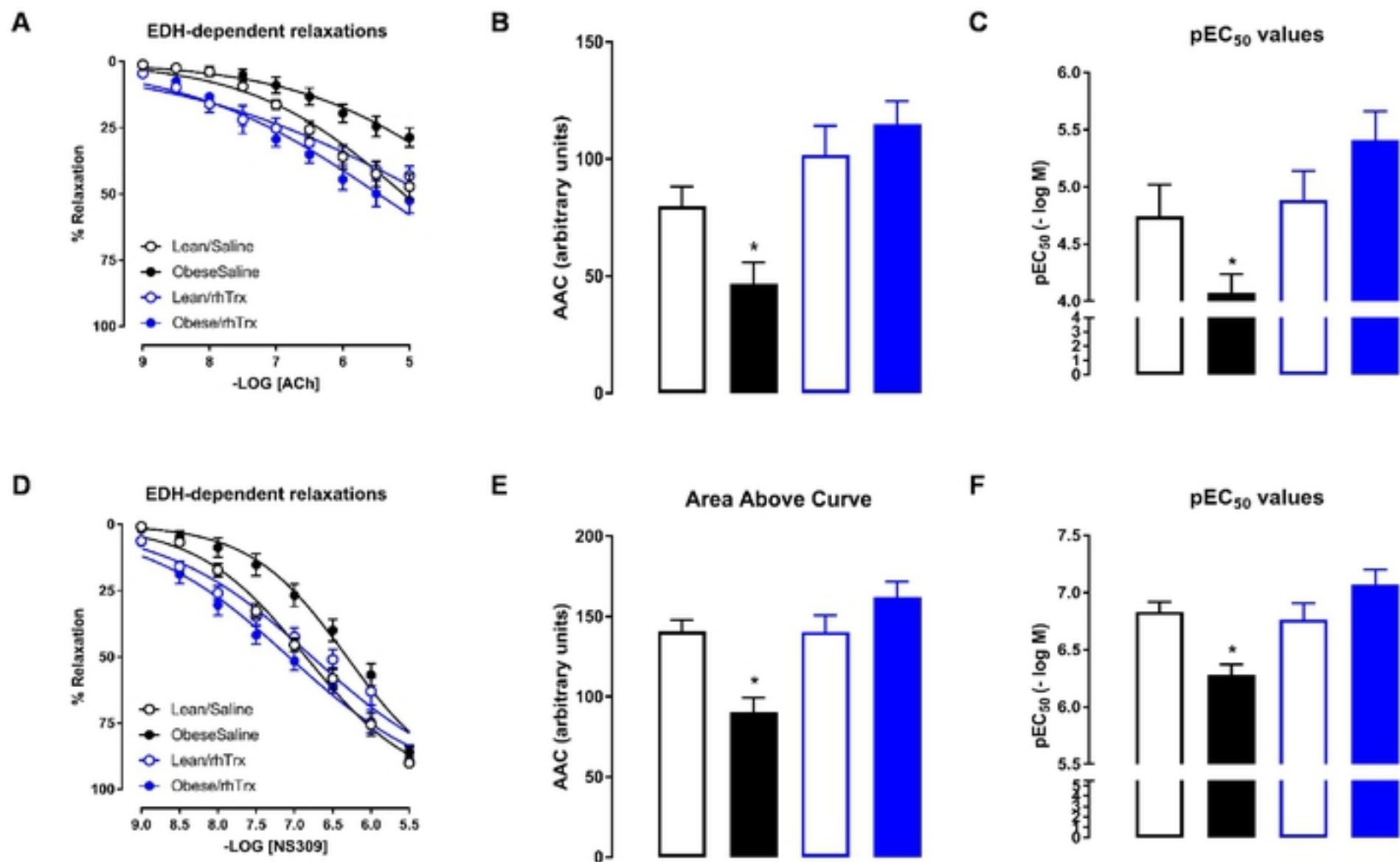


Figure 6